Towards high-frequency negative permeability using magnonic crystals in metamaterial design

M. Mruczkiewicz and M. Krawczyk

Faculty of Physics, Adam Mickiewicz University, Umultowska 85, Poznań 61-614, Poland

R. V. Mikhaylovskiy and V. V. Kruglyak

University of Exeter, Stocker Road, Exeter EX4 4QL, England, United Kingdom

We investigate the magnonic properties of thin slabs of one-dimensional magnonic crystals with the aim of obtaining a structure that possesses negative permeability at high frequencies. Metamaterials of this kind could be used within devices based on the negative refractive index phenomenon. We calculate the relative excitation strengths of different spin-wave modes in one-dimensional magnonic crystals. We find that the coupling between light and high-order magnonic modes can be significant for the specific design of the magnonic structure. These results suggest that magnonic crystals are therefore promising candidates for the negative refractive index metamaterials.

I. INTRODUCTION

In recent years negative refractive index metamaterials have attracted wide attention from researchers.[1,2] Materials possessing simultaneously negative electric permittivity and negative magnetic permeability, and therefore also the negative refractive index (NRI),[3] are desirable due to their unusual electromagnetic properties[4,5] that open ways for creating new potential applications, such as perfect lensing, electromagnetic cloaking, modulators for terahertz radiation, and compact waveguides.[4,6–9] Various methods of realization of metamaterials have been proposed, e.g., based on arrays of split ring resonators[10] or ferromagnetic resonance (FMR) in a magnetic material, where the coupling of light is sufficiently strong to obtain negative permeability in the vicinity of the resonance.[11,12]

The negative refraction of electromagnetic waves due to ferromagnetic resonance has been studied in recent years. It was shown that for the metallic system with a large imaginary part of the dielectric permittivity the negative permeability is a sufficient condition to obtain a negative refraction. For example, the negative refraction was observed in $L_{2/3} Ca_{1/3}MnO_3$ films at 150- and 90-GHz frequencies, under very strong external magnetic fields of over 5 and 3 T, respectively.[13] In ferromagnetic dielectrics, like an yttrium iron garnet (YIG), YIG slabs implanted with metallic wires have been investigated as a NRI (left handed) metamaterial operating in the microwave band.[7] The experimental data were successfully compared with finite element simulations for systems operating in microwave bands from 8 to 18 GHz.[14] Also the periodic structure of interacting nanowires was proposed in Ref. 15 as a metamaterial. The calculations were performed on the basis of an effective permeability tensor for uniform spin-wave excitations, i.e., for FMR conditions.

The FMR in ferromagnetic materials appears usually at GHz frequencies,[11] thereby restricting the possible applications of metamaterials based on this effect to microwaves. Spin-wave resonance (SWR) can extend this limit to frequencies of up to hundreds of GHz, and composites with SWR in THz frequencies are already considered for applications in THz communication. Maxwell equations

simultaneously with the Landau-Lifshitz (LL) equation for the magnetization have been solved to obtain the transmission coefficients for the array of nanowires.[16] Extrema in the transmission function have been found due to spin-wave resonance and antiresonance modes.

A novel design of negative refractive index metamaterial working at sub-THz frequencies was proposed in the recent paper by Mikhaylovskiy *et al.*.[12] The system composed of thin ferromagnetic layers separated by nonmagnetic dielectric material was considered. The significant increase of the resonant frequencies was predicted due to the pinning of the spins on the surfaces of ferromagnetic layers. Here, we propose a different structure to obtain a similar effect. Replacing the uniform ferromagnetic layer by a thin plate of a magnonic crystal[17–20] (MC) will introduce the in-plane quantization of spin-waves.

As a consequence, multiple resonances will be observed in the SWR spectrum in addition to the fundamental uniform excitation. Here we propose to use this effect and we show that coupling of light is strong enough to obtain negative permeability due to the higher-order SWR excitation. We present the method of calculating the scalar permeability function of the extraordinary wave in the case of in-plane magnetization for metamaterials consisting of one-dimensional (1D) magnonic crystals (Fig. 1). Our calculations are based on the plane-wave method (PWM) and analytical formulas for permeability of an effectively uniform magnetic film.[12]

Since the NRI is obtained by SW resonance, the electromagnetic properties of structures proposed in this manuscript will be dependent upon the external magnetic field. The frequency range in which the negative refraction is observed might be tuned by the external magnetic field in a broad frequency range. Structures under consideration will offer some advantages over other NRI metamaterials, and the simplicity, diversity, and versatility of their design might be some of them. A unique functional property of MCs is their re-programmability, i.e., a possibility to obtain the MC in ferromagnetic or antiferromagnetic configuration by manipulation of the bias magnetic field. Then the response of the device will be different in each configuration.[21,22] The intrinsic loss is a factor that might limit the applications of metamaterials.[23,24]
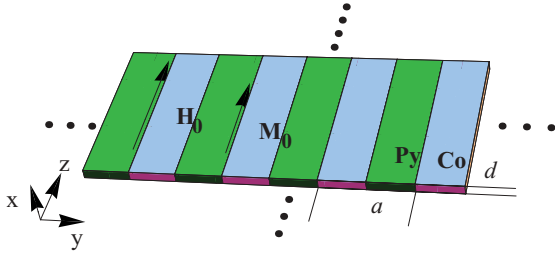
FIG. 1. (Color online) Magnonic crystals considered in this paper: one-dimensional MC of thickness d formed by long stripes of ferromagnetic metals Co and permalloy, arranged with the period a. Bias magnetic field H_0 saturates both materials along the z axis.

However, the metamaterial proposed here might also find an application for developing zero refractive index materials.[25,26] At frequencies larger than the resonance frequency, the magnetic permeability goes from negative to positive values through zero, the latter point called antiresonance condition.[16] Because the antiresonance occurs at frequencies shifted away from the resonances, the absorption decreases.

The paper is organized as follows. In Sec. II the theoretical model is introduced, where the PWM and the calculation method of the relative absorption of electromagnetic waves due to SWRs are presented. In Sec. III the numerical results for one-dimensional MCs are shown and a structure optimized for negative refraction of electromagnetic waves is proposed. The results of calculation of effective parameters, which are used directly to calculate the permeability function, are shown in Sec. IV. The last section is dedicated to conclusions.

II. THEORETICAL MODEL

The band structure of excitations in materials with discrete translational symmetry, including electronic, photonic, phononic, and magnonic crystals, can be calculated by the plane-wave method. The PWM is simple and applicable to any type of periodic arrangement and any shape of scattering centers in bulk samples.[27–31] The PWM has also been used to calculate spin-wave spectra of 1D and two-dimensional (2D) MCs of finite thickness.[32,33] Here we use this technique to calculate the spin-wave spectra of thin plates of 1D MC (as shown in Fig. 1) with the magnetic field in the plane of the MC. Below we outline the method and explain the approximations used. Next, we discuss the method of the calculation of the relative intensities in the SWR spectra from the magnonic profiles found using the PWM method.

A. Plane-wave method

In the continuous medium approach, the spin-wave dispersion relation is determined from the Landau-Lifshitz (LL) equation, i.e., the equation of motion of magnetization vector $\mathbf{M}(\mathbf{r},t)$:

$$\frac{\partial \mathbf{M}(\mathbf{r},t)}{\partial t} = \gamma \mu_0 \mathbf{M}(\mathbf{r},t) \times \mathbf{H}_{\text{eff}}(\mathbf{r},t), \quad (1)$$

where γ is the gyromagnetic ratio and $\mathbf{H}_{\text{eff}}$ denotes the effective magnetic field acting on the magnetization. $\mathbf{r}$ is the position vector and t is the time. The LL equation applies to the case of the absence of dissipation. It is expressed in the International

System of units, used throughout this paper, with μ_0 denoting the permeability of a vacuum. As in the case of free electrons, we will assume $\gamma \mu_0 = 2.21 \times 10^5$ (A/m)$^{-1}$s^{-1}.

In our PWM calculations we shall consider a MC magnetized to saturation, i.e., the case of collinear static magnetization. This allows us to use the linear approximation and a global coordinate system in which the y and z axes define the plane of the MC and the x axis is normal to its surface (Fig. 1). In the case of linear spin waves, the component of the magnetization vector parallel to the static magnetic field (in this study the static magnetic field is assumed to be oriented along the z axis) is constant in time and its magnitude is much greater than that of the perpendicular components: $|\mathbf{m}(\mathbf{r},t)| \ll M_z(\mathbf{r})$ [$\mathbf{M}(\mathbf{r},t) = M_z(\mathbf{r})\hat{\mathbf{z}} + \mathbf{m}(\mathbf{r},t)$, where $\mathbf{m}$ is a two-dimensional vector with components (m_x, m_y)]. Thus, the linear approximation can be applied, by neglecting all the terms with squared $\mathbf{m}(\mathbf{r},t)$ and $\mathbf{h}_{\text{ms}}(\mathbf{r},t)$ (defined below) and assuming $M_z \approx M_S$, M_S being the saturation magnetization, which in the MC is a position-dependent scalar function. We will only search for those solutions of the LL equation that correspond to monochromatic spin waves: $\mathbf{m}(\mathbf{r},t) = \mathbf{m}(\mathbf{r}) \exp(i\omega t)$, ω being the wave frequency.

Effective magnetic field $\mathbf{H}_{\text{eff}}$ acting on the magnetization in an MC is the sum of several components, such as external, exchange, demagnetizing, and anisotropy fields. However, here we shall consider only three: a uniform and constant applied magnetic field $\mathbf{H}_0$ (along the z axis), the exchange field $\mathbf{H}_{\text{ex}}$, and the magnetostatic field $\mathbf{H}_{\text{ms}}$. The latter two fields, i.e., the exchange field and the magnetostatic field, are space dependent:

$$\mathbf{H}_{\text{eff}}(\mathbf{r},t) = \mathbf{H}_0 + \mathbf{H}_{\text{ex}}(\mathbf{r},t) + \mathbf{H}_{\text{ms}}(\mathbf{r},t). \quad (2)$$

We do not take the contribution of the anisotropy field into account, since we do not expect the anisotropy field to have a qualitative influence on the results presented here. In the configuration under consideration, i.e., with $\mathbf{H}_0$ along a stripe axis (see Fig. 1) the shape anisotropy enforces a parallel alignment of all magnetic moments. The exchange field in uniform materials has the well-known form.[34,35] However, in MCs the magnetization changes abruptly at interfaces and a reformulation of the exchange field term is required for the PWM. In the literature different formulations of the exchange field were proposed in calculations of the SW spectra in MCs so far.[30,36,37] Each formulation introduces different boundary conditions on dynamical components of the magnetization vector, so they can describe different physical situations on interfaces. The investigation of these effects requires a further detailed analysis and it is out of the scope of this paper. We assumed the exchange field to have the form that can be obtained directly from the exchange-energy functional in the linear approximation with sharp interfaces:

$$\mathbf{H}_{\text{ex}}(\mathbf{r},t) = \left[\nabla \cdot l_{\text{ex}}^2(\mathbf{r})\nabla\right]\mathbf{m}(\mathbf{r},t), \quad \text{where} \quad l_{\text{ex}} = \sqrt{\frac{2A}{\mu_0 M_S^2}}. \quad (3)$$

In magnetically inhomogeneous materials, the spatial inhomogeneity of both the exchange constant $A(\mathbf{r})$ and the spontaneous magnetization $M_S(\mathbf{r})$ must be taken into account in the definition of the exchange field.

The last component of the effective magnetic field [Eq. (2)], the magnetostatic field is calculated by decomposing this field into the static and dynamic components, $\mathbf{H}_{\mathrm{ms}}(\mathbf{r})$ and $\mathbf{h}_{\mathrm{ms}}(\mathbf{r},t)$, respectively. When the magnetic stripes are infinitely long $\mathbf{H}_{\mathrm{ms}}(\mathbf{r}) = 0$, and this case only is considered in this paper. The time dependence of the dynamic magnetostatic field has the same form as that of the dynamic component of the magnetization vector: $\mathbf{h}_{\mathrm{ms}}(\mathbf{r},t) = \mathbf{h}_{\mathrm{ms}}(\mathbf{r})e^{i\omega t}$.

Using the linear approximation, we derive the following system of equations from Eq. (1):

$$i\frac{\omega}{\gamma\mu_0}m_x(\mathbf{r}) + M_{\mathrm{S}}[\nabla \cdot l_{\mathrm{ex}}^2 \nabla]m_y(\mathbf{r})$$
$$- m_y(\mathbf{r})H_0 + M_{\mathrm{S}}h_{\mathrm{ms},y}(\mathbf{r}) = 0, \qquad (4)$$

$$i\frac{\omega}{\gamma\mu_0}m_y(\mathbf{r}) - M_{\mathrm{S}}[\nabla \cdot l_{\mathrm{ex}}^2 \nabla]m_x(\mathbf{r})$$
$$+ m_x(\mathbf{r})H_0 - M_{\mathrm{S}}h_{\mathrm{ms},x}(\mathbf{r}) = 0. \qquad (5)$$

A and M_{S}, and consequently also l_{ex}^2, are periodic functions of y and constant across the film thickness. The period is equal to a lattice constant a. In MCs composed of two materials, each of these material parameters can be expressed by two values, $M_{\mathrm{S,A}}$, $M_{\mathrm{S,B}}$ and A_{A}, A_{B}, corresponding to each constituent material.

To solve LL Eqs. (4) and (5), we use Bloch's theorem:

$$\mathbf{m}(y) = \sum_G \mathbf{m}_k(G)e^{i(k+G)y}, \qquad (6)$$

where G denotes a reciprocal-lattice vector along the direction of periodicity: $G = \frac{2\pi}{a}n_y$; n_y is an integer. Bloch wave vector k refers to those spin waves that, according to Bloch's theorem, can be limited to the first Brillouin zone (BZ). Already in Eq. (6) we limit ourselves to solutions that are uniform across the film thickness.

In the next step, we perform the Fourier transformation to map the periodic functions M_{S} and l_{ex}^2 to the reciprocal space, as

$$M_{\mathrm{S}}(y) = \sum_G M_{\mathrm{S}}(G)e^{iGy}, \quad l_{\mathrm{ex}}^2(y) = \sum_G l_{\mathrm{ex}}^2(G)e^{iGy}. \quad (7)$$

In the 1D case, the Fourier components of the saturation magnetization $M_{\mathrm{S}}(G)$ and the squared exchange length $l_{\mathrm{ex}}^2(G)$ can be calculated analytically.

We need the formula for the dynamic demagnetizing fields, $h_{\mathrm{ms},x}(y,x)$ and $h_{\mathrm{ms},y}(y,x)$, to finalize the procedure, in which an eigenvalue problem in the reciprocal space is derived from Eqs. (4) and (5). According to the ideas presented in Ref. 38, for a slab of a 2D magnonic crystal with a uniform magnetization along its thickness (its static and dynamic components) Maxwell's equations can be solved in the magnetostatic approximation with the electromagnetic boundary conditions at both surfaces of the slab, i.e., at $x = -d/2$ and $d/2$ (d is a thickness of the MC). For the considered structure, infinite in the (y,z) plane, analytical solutions in the form of a Fourier series can be obtained for dynamic demagnetizing fields:

$$h_{\mathrm{ms},y}(y,x) = \sum_G [im_{x,k}(G) \sinh(|k+G|x)e^{-|k+G|d/2}$$
$$- m_{y,k}(G)(1 - \cosh(|k+G|x)e^{-|k+G|d/2})]$$
$$\times e^{i(k+G)y}, \qquad (8)$$

$$h_{\mathrm{ms},x}(y,x) = \sum_G [im_{y,k}(G) \sinh(|k+G|x)e^{-|k+G|d/2}$$
$$- m_{x,k}(G) \cosh(|k+G|x)e^{-|k+G|d/2}]e^{i(k+G)y}. \qquad (9)$$

Represented in the reciprocal space for the in-plane components, these formulas for the demagnetizing fields are x dependent; i.e., they vary with position across the thickness of the slab. However, when the slab is thin enough (which is the case for the discussed MC, with $d = 5$ nm), the nonuniformity of the demagnetizing fields across its thickness can be neglected, and the respective field values calculated from Eqs. (8) and (9) for $x = 0$ can be used in the PWM calculations. Because of its Fourier series form, the solution found for the demagnetizing fields can be used directly in Eqs. (4) and (5).

The substitution of Eqs. (6)–(9) into Eqs. (4) and (5) leads to the algebraic eigenvalue problem with eigenvalues $i\omega/\gamma\mu_0 H_0$:

$$\hat{M}\mathbf{m}_k = i\frac{\omega}{\gamma\mu_0 H_0}\mathbf{m}_k, \qquad (10)$$

where the eigenvector is $\mathbf{m}_k^{\mathrm{T}} = [m_{x,k}(G_0), \ldots, m_{x,k}(G_N), m_{y,k}(G_0), \ldots, m_{y,k}(G_N)]$ and a finite number N of reciprocal-lattice vectors is used in Fourier series Eqs. (6) and (7). The elements of matrix $\hat{M}$ are defined as

$$\hat{M} = \begin{pmatrix} \hat{M}^{xx} & \hat{M}^{xy} \\ \hat{M}^{yx} & \hat{M}^{yy} \end{pmatrix}. \qquad (11)$$

The submatrices in Eq. (11) are defined as

$$\hat{M}_{ij}^{xx} = -\hat{M}_{ij}^{yy} = -i\frac{1}{H_0}S(k+G_j)M_{\mathrm{S}}(G_i - G_j), \quad (12)$$

$$\hat{M}_{ij}^{xy} = \delta_{ij} + \sum_l \frac{(k+G_j)(k+G_l)}{H_0}l_{\mathrm{ex}}^2(G_l - G_j)M_{\mathrm{S}}(G_i - G_l)$$
$$+ \frac{1}{H_0}[1 - C(k+G_j,x)]M_{\mathrm{S}}(G_i - G_j), \qquad (13)$$

$$\hat{M}_{ij}^{yx} = -\delta_{ij} - \sum_l \frac{(k+G_j) \cdot (k+G_l)}{H_0}l_{\mathrm{ex}}^2(G_l - G_j)$$
$$\times M_{\mathrm{S}}(G_i - G_l) - \frac{1}{H_0}C(k+G_j,x)M_{\mathrm{S}}(G_i - G_j), \quad (14)$$

where indexes of the reciprocal-lattice vectors i, j, and l are integer numbered reciprocal-lattice vectors. The additional functions used in the above equations are defined as follows:

$$S(k,x) = \sinh(|k|x)e^{-|k|d/2},$$
$$C(k,x) = \cosh(|k|x)e^{-|k|d/2}. \qquad (15)$$

We solve the system of Eq. (10) by standard numerical procedures designed for solving complex matrix eigenvalue problems. All the eigenvalues found by these procedures must be tested for convergence, though. A satisfactory convergence of numerical solutions of Eq. (10) for all the structures considered proves to be assured by the use of 101 reciprocal-lattice vectors. The model presented here has been validated by comparison with other numerical simulations and experimental results for MCs composed of Co and permalloy stripes; for details see Ref. 32.

B. Spin-wave profiles and relative SWR intensities

The solution of Eq. (10) yields both eigenfrequencies and corresponding eigenvectors $\mathbf{m}_k(G)$, in the reciprocal space. We determine the corresponding real-space distributions of the eigenmodes using the inverse Fourier transformation given by Bloch's theorem (6). However, to find the response of the magnonic structure to the external uniform ac magnetic field, $\mathbf{b}(t)$, one has to consider the problem of coupling of this field to the eigenmodes of the magnonic crystal. With the spatial profiles of the spin-wave modes at hand, we proceed by calculating relative strengths of the corresponding absorption peaks. The time-averaged absorption power associated with the kth mode $P_k(\mathbf{r})$ at a particular point $\mathbf{r}$ is for a complex vector $\mathbf{m}^*_\mathbf{k}$ given by

$$P_k(\mathbf{r}) = -\frac{1}{T}\int_0^T \mathbf{m}^*_\mathbf{k}(\mathbf{r},t) \cdot \frac{d\mathbf{b}(t)}{dt}\,dt, \tag{16}$$

where $\mathbf{b}(t)$ is the external ac field depending on time, t, and T is the period of its variation. By averaging $P_k(\mathbf{r})$ over the unit cell, we arrive at the absorbed power for the excitation:

$$\langle P(\mathbf{r})\rangle = \frac{1}{V}\int_V P_k(\mathbf{r})\,dV, \tag{17}$$

where V denotes the volume of the unit cell. Thus, the relative efficiency of the interaction of the external uniform ac magnetic field with spin-wave resonances is defined for each mode.

One can see from Eqs. (16) and (17) that only the modes that have a nonzero net dynamic magnetic moment contribute to the absorption and hence can be efficiently excited by the external uniform ac field. In other words, the efficiency of coupling is determined by the overlap integral of the mode and the field profiles.

III. STATIONARY SOLUTIONS IN 1D MAGNONIC CRYSTALS

All calculations in this paper were performed for MC composed of two materials, i.e., cobalt and permalloy. We assumed the following parameters for permalloy: magnetization of saturation $M_S = 0.86 \cdot 10^6$ A/m and exchange constant $A = 1.1 \cdot 10^{-11}$ J/m; for cobalt, $M_S = 1.3 \cdot 10^6$ A/m and $A = 2.8 \cdot 10^{-11}$ J/m. This choice of constituent magnetic materials is not accidental. Recently, there appeared in the literature a few papers on theoretical and experimental investigation of spin waves in thin-film MCs composed of Co and Py stripes with lattice constants of about 500 nm.[32,39,40] The parameters chosen here are taken from Ref. 39, where anisotropy field was neglected, as in our model. This shows also that realization of such MCs is feasible.

The dispersion relation of spin waves in a magnetic film and therefore also in a magnonic crystal is anisotropic.[41,42] It means that the propagation directions parallel and perpendicular to the bias magnetic field are not equivalent. We will limit our investigation to the so-called Damon-Eshbach configuration, i.e., when the wave vector and H_0 are perpendicular to each other.[43] We will consider a SW's propagation along the y axis with a bias magnetic field pointing in the z direction; see Fig. 1. Another important property of SWs is that their dispersion relation is not scalable with the lattice constant, since the relative
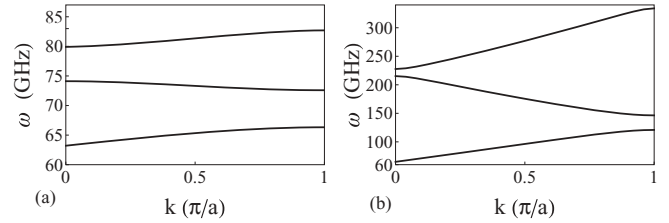
FIG. 2. The dispersion relations of SWs propagating in a 1D MC composed of Co and Py stripes under bias magnetic field $\mu_0 H_0 = 0.01$ T shown for lattice constant of (a) 500 nm and (b) 50 nm.

strength of the exchange and dipolar interactions depends on the lattice-constant value and on the wave vector. For small lattice constants, the onset of the domination of the exchange interaction is expected in the first BZ already, while for large lattice constants the magnetostatic interaction can dominate in the whole first BZ. The exchange interaction is also responsible for increasing frequency of SWs with decreasing lattice constant. The dispersion relations of SWs calculated with the PWM for 1D MCs of 5-nm thickness and lattice constants of 500 and 50 nm are shown in Figs. 2(a) and 2(b), respectively. It is clear that for small a the Brillouin zone is wider and consequently the frequencies of SWs reach higher values.

In Fig. 3, the dispersions of SWs in uniform films of Co (dashed line) and Py (continuous line) are presented as calculated according to the analytical formula from Ref. 44. On the same graph, the vertical dashed lines indicate that the BZ edges occurred for the MC with the periodicity of $a = 50$ and 500 nm. We can see that, for small a, e.g., 50 nm, the dispersion has a parabolic shape for wave vectors at the edge of the BZ, while for large a, e.g., 500 nm, it is almost linear. The SW resonances at high frequencies in the center of the BZ appear due to introducing the periodicity. Band folding for SWs with dominating exchange interactions will appear at large wave vectors. It means that for high-frequency applications the MCs with small lattice constants are more suitable; see Fig. 4. The frequencies of SWs in 1D MCs with the wave vector equal to
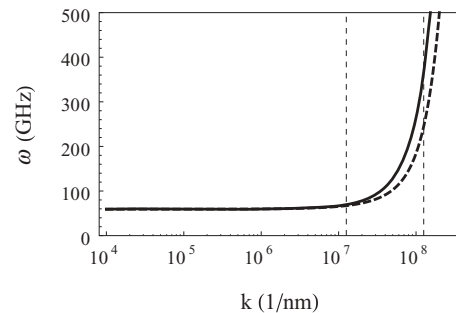
FIG. 3. The dispersion relation of SW propagating in a thin uniform magnetic film under bias field $\mu H_0 = 0.1$ T for Co (dashed line) and Py (continuous line). The grid lines indicate the values of the wave vector (in logarithmic scale) at the second Brillouin-zone edge of a lattice constant of 500 nm ($k = 1.26 \cdot 10^7$ 1/m) and 50 nm ($k = 1.26 \cdot 10^8$ 1/m). Values of frequencies at these points are in the range of frequencies of the second-order mode, appearing due to the periodicity, in MC. This explains the increase of the SW mode frequencies with decrease of the lattice constant of the magnonic crystal observed in Figs. 2 and 4.
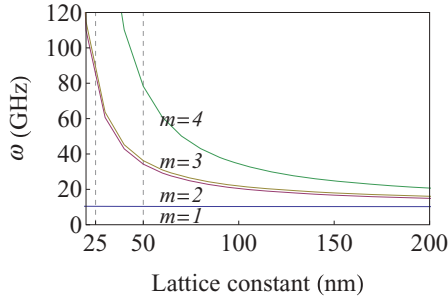
FIG. 4. (Color online) Dependence of the frequency of SWs on the lattice constant of a 1D MC. The frequencies of spin waves at the center of the first BZ are shown. m indicates the mode (band) number. The structure is composed of alternating cobalt and permalloy stripes of 5-nm thickness with the width varied from 10 to 100 nm; i.e., the lattice constant varies from 20 to 200 nm. The frequencies of modes above the first one increase as the lattice constant decreases. This effect is crucial to our work and indicates the importance of using the MC with small lattice constants.

zero are plotted as a function of the lattice constant. We find that the frequency of the first band is only weakly dependent on a while frequencies of higher bands significantly increase with frequency; e.g., the second band for a 50-nm lattice constant has a frequency already close to 40 GHz.

We show the SWR calculated for a Co and Py MC in Fig. 5(a). The relatively high intensity of the third resonant mode is visible. The reason for its high intensity could be understood by looking at the profiles of SWs shown in Figs. 5(b)–5(d). The distribution of the dynamical component of the magnetization is not symmetric among Co and Py. The highest amplitude of the m_x component is localized within the permalloy stripes for the first mode and within the cobalt stripes for the third mode. In the case of the second and fourth modes, the distribution has an antisymmetrical character, so they do not efficiently couple with the electromagnetic wave.
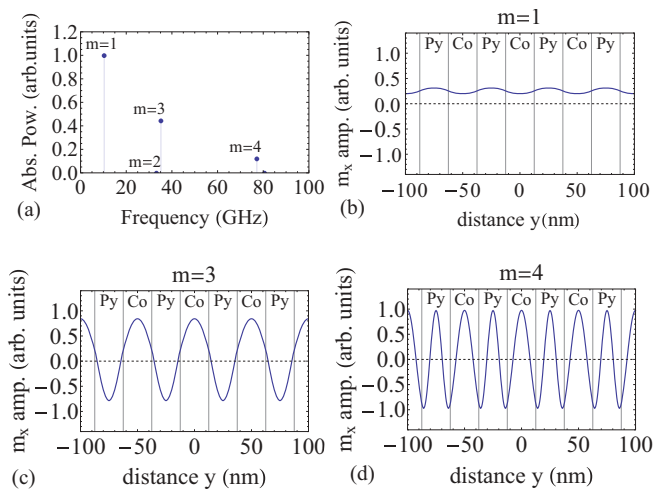
FIG. 5. (Color online) The analysis of the resonant modes of 1D magnonic crystal composed of alternating cobalt and permalloy stripes of 25-nm width each and 5-nm thickness. The graphs show (a) the relative absorption intensities and (b–d) The distribution of the x component of dynamic magnetization for modes with $m = 1$, 3, and 4.

IV. EFFECTIVE PARAMETERS AND PERMEABILITY OF 1D MC

In the long-wavelength limit when the length of the material modulation is much shorter than the wavelength of SWs, the magnonic crystal appears to have properties of a uniform material. In this limit, such effective parameters as the magnetization saturation, exchange coefficient, and magnetic field can be assigned to the magnonic metamaterial and describe SWs in it. The proper assignment of the effective parameters is not a simple task because it depends on the scale and the structure of the MC. In the 2D case of MC formed by an antidot lattice (ADL), it was shown that long SWs behave either as in effective waveguides or as in uniform thin film.[45,46] This depends on the symmetry of the antidot lattice and on the filling fraction, i.e., the relative space occupied by antidots in a magnetic material. In an MC formed by ferromagnetic materials only, the SW should behave as in a uniform thin film with effective values of the magnetization saturation and effective exchange constant in the long-wave limit.

The effective parameters could be extracted from a dispersion relation so that when they are applied in the analytical formula for the dispersion relation the function is reconstructed.[47–49] For our purposes it seems better to do it in a different way, since we are interested in magnonic properties exactly at $k = 0$, i.e., under the SWR condition. In particular, the exchange constant has no effect on the position of the first resonance peak. So, we propose to extract the value of the effective saturation magnetization by fitting the spin-wave frequency to the following analytical formula as a function of the bias magnetic field, H_0, in the homogeneous thin film, i.e., the Kittel formula:[41]

$$\omega(H_0) = \gamma \mu_0 \sqrt{[H_0(H_0 + M_{eff})]}, \qquad (18)$$

with numerical results of the PWM obtained by solving Eq. (10). In Eq. (18), M_{eff} is the effective saturation magnetization. In Fig. 6, the continuous line represents function $\omega(H_0)$ obtained from numerical solution of Eq. (10). By fitting M_{eff} in Eq. (18), we found effective magnetization $M_{eff} = 1.0 \cdot 10^6$ A/m. This value is very close to the weighted average of magnetization in Co and Py, $M_{av} = 1.08 \cdot 10^6$ A/m. The dependence of the first resonance frequency upon the bias
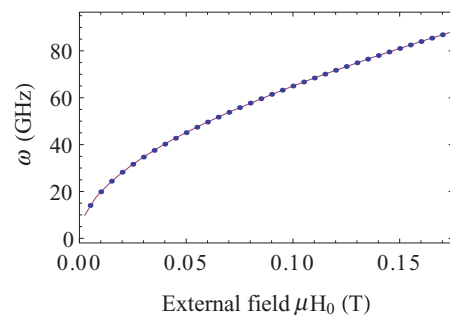
FIG. 6. (Color online) The first resonant frequency of the 1D MC composed of alternating cobalt and permalloy stripes of 25-nm width each (5-nm thicknesses) plotted as a function of the external magnetic field using the analytical formula, where the effective magnetization is a parameter (continuous line), and from the results of PWM for Co and Py magnonic crystal (dots).
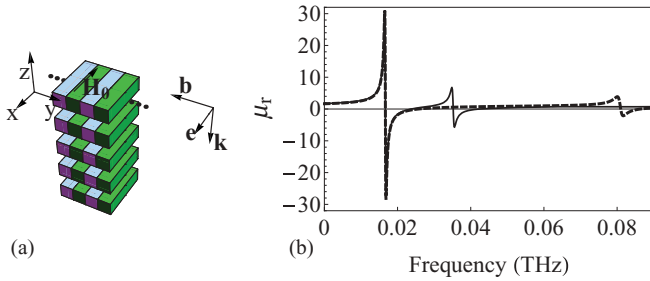
FIG. 7. (Color online) (a) The structure of the metamaterial under investigation. **e**, **b** indicates the polarizations of external electric and magnetic fields, and **k** indicates the direction of propagation. (b) The real part of permeability calculated according to Eq. (21) (μ_r) as a function of a frequency for the stack of thin layers made of slabs of 1D MC, composed of alternating 5-nm-thick cobalt and permalloy stripes of 25-nm width (solid line) and 12.5-nm width (dashed line) under the influence of the external magnetic field of $H_0 = 0.2$ T. The filling fraction of the magnonic crystal in the nonmagnetic dielectric matrix is 25%, the same as in Ref. 12.

magnetic field given by Eq. (18) with the fitted value of the effective magnetization is superimposed on the PWM results and marked by dots. The relative error is small and does not exceed 1.5% in the range of bias magnetic fields from 0 to 0.2 T.

Using the results from PWM, we propose to create a metamaterial with negative permeability. Our idea is based on the model developed by Mikhaylovskiy *et al.*,[12] where a stack of thin ferromagnetic films separated by nonmagnetic dielectric layers was proposed as a metamaterial. The effective negative permeability was obtained in the proximity of the SWR frequencies in a sub-THz range. The relatively high frequencies resulted from standing waves formed across the thickness of the thin ferromagnetic films. Here, we propose another method of shifting SWR to higher frequencies by introducing thin MC slabs instead of the uniform thin films. A schematic drawing of the proposed structure is shown in Fig. 7(a). The SWR resonance at high frequencies is achieved now due to the lateral (in-plane) quantization of spin waves, while uniform excitations are assumed across the thickness. Below, we describe our idea in detail together with estimations of the permeability of such a structure. According to the PWM results we expect the values of the higher resonant frequencies to increase with the decrease of the lattice constant; see Fig. 4. This dependence gives an opportunity to design the structure of MC according to a required frequency range of negative permeability.

Having M_{eff} at hand we can plot the permeability as a function of frequency by using the analytical solution derived in Ref. 12 for the material that is characterized by this effective magnetization. This analytical solution for the $\mu(\omega)$ in the vicinity of the frequency of the first resonance can be fitted with the resonance formula:[42]

$$\mu(\omega) = 1 + \frac{A_1}{\omega_1 - \omega + i\omega\alpha},\tag{19}$$

where A_1 is a fitting parameter and ω_1 is the first SWR frequency. In order to find the absolute value of an absorbed power at higher resonant frequencies we normalize their relative intensities (found in PWM) to A_1, so the relative intensities of the first three modes for an MC with a 50-nm

lattice constant are now

$$A_1 = 0.0058, \quad A_2 = 1.16 \cdot 10^{-13} \cdot A_1 \approx 0,$$
$$A_3 = 0.45 \cdot A_1.\tag{20}$$

The permeability function can be obtained now by using frequencies and intensities from the normalized absorption of peaks calculated with the PWM as

$$\mu(\omega) = 1 + \sum_{j=1}^{N} \frac{A_j}{\omega_j - \omega + i\omega\alpha},\tag{21}$$

where A_j are the parameters that describe the intensities of the permeability function already found in Eq. (20) and ω_j are the resonant frequencies of the 1D MC (known from PWM calculations). N is the number of modes, which in our consideration is restricted to 3. The resulting real part of function $\mu(\omega)$ is shown in Fig. 7(b) by a solid line. The value of the damping factor, α, is taken as $\alpha = 0.01$. We assume the same composition of the metamaterial as in Ref. 12 but instead of the uniform ferromagnetic films we include 1D MCs. The MC occupies 25% of the volume, while the rest is nonmagnetic dielectric [see Fig. 7(a)]. This solution is obtained for the geometry where the external magnetic field is applied in the plane of the magnetic film. The propagating wave is linearly polarized, perpendicular to the magnetic field [see Fig. 7(a) for the orientation of the ac magnetic field and wave propagating direction]. The wavelength of the electromagnetic wave is much longer than the thickness of the film, and so the electromagnetic field is assumed to be uniform in a single film made of 1D MC. In the MC, due to the periodicity in the structure the band folding effect is observed, and many resonances might be observed at higher frequencies for $k = 0$.

In Fig. 7(b) we showed that the relative absorption intensity of the higher modes of the thin slab of magnonic crystal can be comparable with that of the first mode and thus lead to a significant absorption due to the spin-wave resonances. As a result the proposed metamaterial can have a negative permeability at elevated frequencies as shown in Fig. 7(b).

We can increase the frequency of SWR and the frequency of the NRI band more by increasing an external magnetic field or by decreasing a lattice constant. In Fig. 4 was shown the increase of SWR frequencies (for $m > 1$) with decreasing lattice constant. In Fig. 7(b) by the dashed line we show the permeability in the function of frequency for an MC composed of Co and Py stripes of 12.5-nm width. The band of negative permeability connected with the second mode still exists at frequencies above 80 GHz.

Finally, it is instructive to estimate the figure of merit (FOM) of the proposed metamaterial, defined as

$$\text{FOM} = -\frac{\text{Re}(n)}{\text{Im}(n)},\tag{22}$$

where n is defined according to Ref. 52, fulfilling the causality principle. First, one should find the effective permittivity of the single magnonic crystal $\varepsilon_{\text{eff}}^{\text{MC}}$. In the case of normal incidence of light the permittivity can be approximated by[50]

$$\frac{1}{\varepsilon_{\text{eff}}^{\text{MC}}} = \frac{f_{\text{Co}}}{\varepsilon_{\text{Co}}} + \frac{f_{\text{P}}}{\varepsilon_{\text{P}}},\tag{23}$$
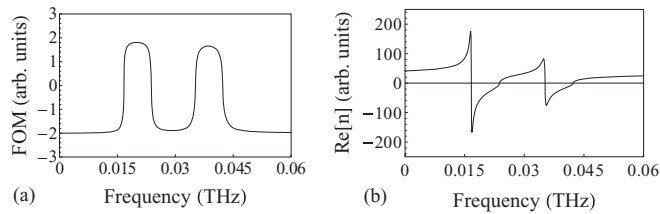
FIG. 8. (a) Figure of merit (FOM) in the function of a frequency of the considered metamaterial (the stack of thin layers made of slabs of 1D MC, composed of alternating 5-nm-thick cobalt and permalloy stripes of 25-nm width) with negative refractive index. (b) The real part of the refractive index.

where f_{Co}, ε_{Co}, f_P, and ε_P are the relative volume fraction and permittivity of cobalt and permalloy, respectively. Structures considered here have $f_{Co} = f_{Co} = 0.5$. Then the effective permittivity of the whole structure is

$$\varepsilon_{\text{eff}} = (1 - \rho)\varepsilon_{\text{h}} + \rho\varepsilon_{\text{eff}}^{\text{MC}}, \quad (24)$$

where ε_{h} is the permittivity of the host nonmagnetic dielectric and ρ denotes the filling factor of the magnonic plates in the metamaterial, $\rho = 0.25$. We assume $\varepsilon_{Co} \approx \varepsilon_{Py} \approx (-1 - i) \cdot 10^4 \gg \varepsilon_{\text{h}}$.[51] Thus we arrive at the simple estimate for the effective permittivity as $\varepsilon_{\text{eff}} = \rho\varepsilon_{Co(Py)}$. The FOM for a metamaterial composed of 1D MCs with Co and Py stripes of 25-nm width is shown in Fig. 8(a), and the real part of the refractive index is shown in Fig. 8(b). We can see that the FOM in the frequencies around the negative refractive index (i.e., around 15 and 37 GHz) reaches the value of 2.

The values of the FOM found at resonant frequencies in this work are comparable with values found for fishnet structures proposed in Ref. 53 and lower than those found in Ref. 54, where the coupling relationship between the electric and magnetic resonances was studied in double bowknot shaped structures in order to optimize losses. The authors of Ref. 55 propose a structure that does not contain any metallic materials but a cubic periodic array of layered dielectric spheres, made from low-loss high-permittivity ceramics. Since the absorption is much lower in dielectrics, they achieve a low-loss NRI material. In MC based metamaterials considered here there are a few ways for improving the FOM. Instead of the ferromagnetic metals we can consider a dielectric ferromagnet (e.g., yttrium iron garnet) as a basis for the

proposed structures. Another way for decreasing loss is to remove one of the magnetic metallic materials or to use two-dimensional antidot lattices (ADLs) as the 1D MCs. In both cases we can expect the effect of periodicity and in-plane quantization to remain.[21,22,45,56] The ADLs formed by a regular lattice of holes in the thin film of ferromagnetic material have been intensively studied recently and the formation of a magnonic band structure was experimentally proved.[57–59]

V. CONCLUSIONS

We demonstrate that negative permeability at frequencies close to 100 GHz can be achieved in the periodic metallic magnetic structures, i.e., thin plates of 1D magnonic crystals, being a result of the lateral quantization of SWs. We investigate the frequencies of the resonant modes of MCs as well their relative absorption intensities in dependence on the lattice constant. The analysis of the mode profiles is conducted in order to demonstrate the strong coupling of high-order magnonic modes to electromagnetic waves. We showed that for the structure composed of the stack of thin films of 1D MCs with lattice constants of 50 and 25 nm (i.e., alternating cobalt and permalloy stripes with a thickness of 5 nm and a width of 25 or 12.5 nm) separated with a nonmagnetic dielectric, negative permeability can be achieved at relatively high frequencies. We expect that further decreasing the lattice constant or introducing periodicity in the second dimension should shift SWR and so bands of a negative permeability above 100 GHz. Other possibilities for increasing the resonant frequencies of SW modes are increasing the field or using the antidot systems, but for the antidot applications further research is necessary. There is also a possibility of applying the pinning boundary conditions on the top or bottom surfaces of the thin plate of the MC. In this case the combined effects of the lateral and thickness quantization of SW modes should result in increasing frequencies of SWR above 100 GHz.

ACKNOWLEDGMENTS

[1]A. De Baas (ed.), *Nanostructured Metamaterials* (Publications Office of the European Union, Luxembourg, 2010).

[2]Y. Liu and X. Zhang, Chem. Soc. Rev. **40**, 2494 (2011).

[3]V. G. Veselago, Sov. Phys. Usp. **10**, 509 (1968).

[4]J. B. Pendry, D. Schurig, and D. R. Smith, Science **312**, 1780 (2006).

[5]N. Engheta and R. Ziolkowski, IEEE Trans. Microwave Theory Tech. **53**, 1535 (2005).

[6]J. B. Pendry, Phys. Rev. Lett. **85**, 3966 (2000).

[7]H. Zhao, J. Zhou, Q. Zhao, B. Li, L. Kang, and Y. Bai, Appl. Phys. Lett. **91**, 131107 (2007).

[8]H.-T. Chen, J. F. O'Hara, A. K. Azad, A. J. Taylor, R. D. Averit, D. B. Shrekenhamer, and W. J. Padilla, Nature Phot. **2**, 295 (1998).

[9]A. Alú and N. Engheta, IEEE Trans. Microwave Theory Tech. **52**, 199 (2004).

[10]J. B. Pendry, A. J. Holden, D. J. Robbins, and W. J. Stewart, IEEE Trans. Microwave Theory Tech. **47**, 2075 (1999).

[11]O. Acher, J. Magn. Magn. Mater. **321**, 2093 (2009).

[12]R. V. Mikhaylovskiy, E. Hendry, and V. V. Kruglyak, Phys. Rev. B **82**, 195446 (2010).

[13]A. Pimenov, A. Loidl, K. Gehrke, V. Moshnyaga, and K. Samwer, Phys. Rev. Lett. **98**, 197401 (2007).

[14] J. Carbonell, H. García-Miquel, and J. Sánchez-Dehesa, Phys. Rev. B **81**, 024401 (2010).

[15] V. Boucher and D. Ménard, Phys. Rev. B **81**, 174404 (2010).

[16] M. Pardavi-Horvath, G. S. Makeeva, and O. A. Golovanov, IEEE Trans. Magn. **47**, 313 (2011).

[17] S. Neusser and D. Grundler, Adv. Mater. **21**, 2927 (2009).

[18] V. V. Kruglyak, S. O. Demokritov, and D. Grundler, J. Phys. D: Appl. Phys. **43**, 264001 (2010).

[19] A. A. Serga, A. V. Chumak, and B. Hillebrands, J. Phys. D: Appl. Phys. **43**, 264002 (2010).

[20] B. Lenk, H. Ulrichs, F. Garbs, and M. Mnzenberg, Phys. Rep. **507**, 107 (2011).

[21] S. Tacchi, M. Madami, G. Gubbiotti, G. Carlotti, S. Goolaup, A. O. Adeyeye, N. Singh, and M. P. Kostylev, Phys. Rev. B **82**, 184408 (2010).

[22] G. Duerr, R. Huber, and D. Grundler, J. Phys.: Condens. Matter **24**, 024218 (2012).

[23] J. T. Shen and P. M. Platzman, Appl. Phys. Lett. **80**, 3286 (2002).

[24] D. R. Smith, D. Schurig, M. Rosenbluth, S. Schultz, S. Anantha Ramakrishna, and J. B. Pendry, Appl. Phys. Lett. **82**, 1506 (2003).

[25] R. W. Ziolkowski, Phys. Rev. E **70**, 046608 (2004).

[26] S. Kocaman, M. S. Aras, P. Hsieh, J. F. McMillan, C. G. Biris, N. C. Panoiu, M. B. Yu, D. L. Kwong, A. Stein, and C. W. Wong, Nature Photonics **5**, 499 (2011).

[27] J. D. Joannopoulos, R. D. Meade, and J. N. Winn, *Photonic Crystals: Molding the Flow of Light*, 2nd ed. (Princeton University Press, Princeton, 2008).

[28] D. W. Prather, S. Shi, A. Sharkawy, J. Murakowski, and G. J. Schneider, *Photonic Crystals: Theory, Applications, and Fabrication* (Wiley, New York, 2009).

[29] V. Laude, M. Wilm, S. Benchabane, and A. Khelif, Phys. Rev. E **71**, 036607 (2005).

[30] M. Krawczyk and H. Puszkarski, Phys. Rev. B **77**, 054437 (2008).

[31] J. O. Vasseur, P. A. Deymier, B. Djafari-Rouhani, Y. Pennec, and A.-C. Hladky-Hennion, Phys. Rev. B **77**, 085415 (2008).

[32] M. L. Sokolovskyy and M. Krawczyk, J. Nanopart. Res. **13**, 6085 (2011).

[33] J. W. Klos, M. Krawczyk, and M. L. Sokolovskyy, J. Appl. Phys. **109**, 07D311 (2011).

[34] A. I. Akhiezer, V. G. Baryachtar, and S. V. Peletminsky, *Spin Waves* (North-Holland, Amsterdam, 1968).

[35] S. Chikazumi, *Physics of Ferromagnetism* (Oxford Press, Oxford, 1997).

[36] J. O. Vasseur, L. Dobrzynski, B. Djafari-Rouhani, and H. Puszkarski, Phys. Rev. B **54**, 1043 (1996).

[37] V. V. Kruglyak, A. N. Kuchko, and V. I. Finokhin, Phys. Sol. State **46**, 842 (2004).

[38] J. Kaczer and L. Murtinova, Phys. Status Solidi A **23**, 79 (1974).

[39] Z. K. Wang, V. L. Zhang, H. S. Lim, S. C. Ng, M. H. Kuok, S. Jain, and A. O. Adeyeye, Appl. Phys. Lett. **94**, 083112 (2009).

[40] Z. K. Wang, V. L. Zhang, H. S. Lim, S. C. Ng, M. H. Kuok, S. Jain, and A. O. Adeyeye, ACS Nano **4**, 643 (2010).

[41] D. D. Stancil and A. Prabhakar, *Spin Waves* (Springer, New York, 2009).

[42] A. G. Gurevich and G. A. Melkov, *Magnetization Oscillations and Waves* (CRC, Boca Raton, 1996).

[43] R. W. Damon and J. R. Eshbach, J. Phys. Chem. Solids **19**, 308 (1961).

[44] B. A. Kalinikos and A. N. Slavin, J. Phys. C **19**, 7013 (1986).

[45] S. Neusser, G. Duerr, S. Tacchi, M. Madami, M. L. Sokolovskyy, G. Gubbiotti, M. Krawczyk, and D. Grundler, Phys. Rev. B **84**, 094454 (2011).

[46] S. Neusser, H. G. Bauer, G. Duerr, R. Huber, S. Mamica, G. Woltersdorf, M. Krawczyk, C. H. Back, and D. Grundler, Phys. Rev. B **84**, 184411 (2011).

[47] S. Datta, C. T. Chan, K. M. Ho, and C. M. Soukoulis, Phys. Rev. B **48**, 14936 (1993).

[48] A. A. Krokhin, P. Halevi, and J. Arriaga, Phys. Rev. B **65**, 115208 (2002).

[49] Y. Wu, Y. Lai, and Z.-Q. Zhang, Phys. Rev. B **76**, 205313 (2007).

[50] R. W. Boyd, R. J. Gehr, G. L. Fischer, and J. E. Sipe, Pure Appl. Opt. **5**, 505 (1996).

[51] M. A. Ordal, L. L. Long, R. J. Bell, S. E. Bell, R. R. Bell, R. W. Alexander Jr., and C. A. Ward, Appl. Opt. **22**, 1099 (1983).

[52] R. W. Ziolkowski and E. Heyman, Phys. Rev. E **64**, 056625 (2001).

[53] C. Sabah and H. G. Roskos, J. Phys. D: Appl. Phys. **44**, 255101 (2011).

[54] X. Zhou, Y. Liu, and X. Zhao, Appl. Phys. A **98**, 643 (2010).

[55] E. F. Kuester, N. Memic, S. Shen, A. Scher, S. Kim, K. Kumley, and H. Loui, Progress In Electromagnetics Research B **33**, 175 (2011).

[56] A. Barman, J. Phys. D: Appl. Phys. **43**, 195002 (2010).

[57] S. L. Vysotski, S. A. Nikitov, and Y. A. Filimonov, J. Exp. Theor. Phys. **101**, 547 (2005).

[58] S. Neusser, G. Durr, H. G. Bauer, S. Tacchi, M. Madami, G. Woltersdorf, G. Gubbiotti, C. H. Back, and D. Grundler, Phys. Rev. Lett. **105**, 067208 (2010).

[59] R. Zivieri, S. Tacchi, F. Montoncello, L. Giovannini, F. Nizzoli, M. Madami, G. Gubbiotti, G. Carlotti, S. Neusser, G. Duerr, and D. Grundler, Phys. Rev. B **85**, 012403 (2012).